Asociación Argentina
de Mecánica Computacional

Mecánica Computacional Vol XXXVII, págs. 931-941 (artículo completo)
A. Cardona, L. Garelli, J.M. Gimenez, P.A. Kler, S. Márquez Damián, M.A. Storti (Eds.)
Santa Fe, 5-7 Noviembre 2019

A FULLY DISCRETE ADAPTIVE SCHEME FOR PARABOLIC EQUATIONS

Eduardo M. Garau[a], Fernando D. Gaspoz[b], Pedro Morin[a] and Rafael Vázquez[c,d]

[a] *Universidad Nacional del Litoral, Consejo Nacional de Investigaciones Científicas y Técnicas, FIQ, Santa Fe, Argentina, eduardogarau@gmail.com, morinpedro@gmail.com*

[b] *Technische Universität Dortmund, Fakultät für Mathematik, Vogelpothsweg 87, 44227 Dortmund, Germany, fernando.gaspoz@tu-dortmund.de*

[c] *Institute of Mathematics, Ecole Polytechnique Fédérale de Lausanne, Station 8, 1015 Lausanne, Switzerland, rafael.vazquez@epfl.ch*

[d] *Istituto di Matematica Applicata e Tecnologie Informatiche "E. Magenes" del CNR, Via Ferrata 1, 27100 Pavia, Italy*

Keywords: adaptivity, parabolic equations, convergence into tolerance, B-splines

Abstract. We present an adaptive algorithm for solving linear parabolic equations using hierarchical B-splines and the implicit Euler method for the spatial and time discretizations, respectively. Our development improves upon one from 2018 from Gaspoz and collaborators, where fully discrete adaptive schemes have been analyzed within the framework of classical finite elements. Our approach is based on an a posteriori error estimation that essentially consists of four indicators: a time and a consistency error indicator that dictate the time-step size adaptation, and coarsening and a space error indicator that are used to obtain suitably adapted hierarchical meshes (at different time-steps). Even though we use hierarchical B-splines for the space discretization, a straightforward generalization to other methods, such as FEM, is possible. The algorithm is guaranteed to reach the final time within a finite number of operations, and keep the space-time error below a prescribed tolerance. Some numerical tests document the practical performance of the proposed adaptive algorithm.

1 INTRODUCTION

In this article we propose an adaptive method for solving numerically equations of the type:

$$\begin{cases} u_t + \mathcal{L}u = f \quad \text{in} \quad \Omega_T, \qquad u = 0 \quad \text{on} \quad \partial\Omega \times (0,T) \\ u(\cdot,0) = u_0 \quad \text{in} \quad \Omega \end{cases} \tag{1.1}$$

where $\Omega \subset \mathbb{R}^d$ is a Lipschitz domain, $T > 0$, $\Omega_T = \Omega \times (0,T)$, $f \in L^2(\Omega_T) = L^2(0,T;L^2(\Omega))$, $u_0 \in L^2(\Omega)$ and $\mathcal{L}$ denotes the second order elliptic operator $\mathcal{L}u = -\operatorname{div}(\mathcal{A}\nabla u) + cu$, with $\mathcal{A} : \Omega \to \mathbb{R}^d \times \mathbb{R}^d$ smooth, symmetric and uniformly elliptic, and $c \in L^\infty(\Omega)$ is nonnegative.

For the spatial error estimation we use the function based a posteriori error indicators for hierarchical B-spline discretizations of elliptic problems introduced in Buffa and Garau (2018) and follow the ideas in Kreuzer et al. (2012) and Gaspoz et al. (2018) for the design of the time stepping adaptive method, which we improve in several aspects. We use the data structures and some algorithms from Garau and Vázquez (2018) for the implementation.

In this article we will present the main ideas leading to the adaptive algorithm and its analysis, and leave the details and most proofs to a forthcoming paper.

2 PROBLEM SETTING

We now introduce the *weak formulation* of problem (1.1). Let $\mathbb{V} := H^1_0(\Omega)$ and $B : \mathbb{V} \times \mathbb{V} \to \mathbb{R}$ be the bilinear form associated to the operator $\mathcal{L}$:

$$B[u,v] = \int_\Omega \mathcal{A}\nabla u \cdot \nabla v + cuv, \qquad \forall u, v \in \mathbb{V}. \tag{2.1}$$

Let

$$\mathbb{W}(0,T) := \{u \in L^2(0,T;H^1_0(\Omega)) \mid \partial_t u \in L^2(0,T;H^{-1}(\Omega))\}, \tag{2.2}$$

which is a Banach space equipped with norm $\|v\|^2_{\mathbb{W}(0,T)} := \int_0^T (\|\partial_t v\|^2_{H^{-1}(\Omega)} + |||v|||^2)\, dt + \|v(T)\|_{L^2(\Omega)}$, where $|||v|||^2 := B[v,v]$ and $\|g\|_{H^{-1}(\Omega)} := \sup_{v \in H^1_0(\Omega)} \frac{\langle g, v\rangle}{|||v|||}$.

We say that $u \in \mathbb{W}(0,T)$ is a weak solution of (1.1) if

(i) $\langle \partial_t u(t), v\rangle + B[u(t),v] = \langle f(t), v\rangle_\Omega, \quad \forall\, v \in \mathbb{V}$ and a.e. $t \in (0,T)$,

(ii) $u(0) = u_0$. (This equality is well defined because $\mathbb{W}(0,T) \subset C([0,T];L^2(\Omega))$).

3 SPACE-TIME DISCRETIZATION

The adaptive algorithm produces a partition $0 = t_0 < t_1 < \cdots < t_N = T$ of the time interval into subintervals $I_n = [t_{n-1}, t_n]$ with corresponding local time-step sizes $\tau_n = |I_n| = t_n - t_{n-1}$, $n = 1, 2, \ldots, N$, which are obtained adaptively.

The algorithm starts with $U_0 = U_0^* \in \mathbb{V}_0^* = \mathbb{V}_0$, an approximation of the initial value u_0, where $\mathbb{V}_0^*$ is a finite dimensional subspace of $H^1_0(\Omega)$. In this article we will work with hierarchical spline spaces $\mathbb{V}_n := \operatorname{span} \mathcal{H}_n$ with $\mathcal{H}_n$ a hierarchical B-spline basis associated to a hierarchical mesh $\mathcal{Q}_n$ defined in Ω; but there is no essential impediment to work with other discretizations offering the possibility to perform adaptivity through refinement and coarsening.

For each $n \in \mathbb{N}$, the algorithm then leads to a space $\mathbb{V}_n \supset \mathbb{V}^*_{n-1}$ and computes $U_n \in \mathbb{V}_n$ as the solution of the following modified implicit Euler scheme :

$$\frac{1}{\tau_n}\langle U_n - U^*_{n-1}, V\rangle_\Omega + B[U_n, V] = \langle f_n, V\rangle_\Omega, \quad \forall\, V \in \mathbb{V}_n, \qquad \text{with } f_n := \fint_{I_n} f(t)\, dt. \tag{3.1}$$

Once $U_n \in \mathbb{V}_n$ has been computed, the algorithm adaptively coarsens the space $\mathbb{V}_n$ leading to a space $\mathbb{V}_n^* \subset \mathbb{V}_n$ and a still suitable representation $U_n^* \in \mathbb{V}_n^*$ of U_n; the goal of this coarsening step is to reduce the amount of data used to store U_n, while keeping a good approximation.

Notice that choosing U_n^* as the L^2-projection of U_n onto $\mathbb{V}_n^*$ we obtain the method presented in Kreuzer et al. (2012); Gaspoz et al. (2018). However, we do not recompute U_n^* when the space $\mathbb{V}_{n+1}$ is being obtained through refinement of $\mathbb{V}_n^*$, nor we store $\mathcal{Q}_n$ in memory to keep full information of U_n. We only need to store U_n^* in the hierarchical space associated to $\mathcal{Q}_n^*$ and refine this mesh to obtain $\mathcal{Q}_{n+1}$ and the corresponding space $\mathbb{V}_{n+1}$. This is an essential advantageous difference to Kreuzer et al. (2012); Gaspoz et al. (2018).

In order to measure the error we define the discrete solution $\mathcal{U} \in \mathbb{W}(0,T)$ as

$$\mathcal{U}(t) := \frac{t - t_{n-1}}{\tau_n} U_n + \frac{t_n - t}{\tau_n} U_{n-1}, \qquad \text{for } t \in I_n, \quad n = 1, \dots, N. \tag{3.2}$$

4 A POSTERIORI ERROR ESTIMATION: UPPER BOUND FOR THE ERROR

The adaptive algorithm is based on the following *a posteriori* error indicators:

- **Initial error indicator:** $\mathcal{E}_0^2 = \|U_0 - u_0\|^2_{L^2(\Omega)}$.
- **Coarsening error indicator:** $\mathcal{E}_c^2(n) = 2\tau_n \left|\!\left|\!\left| U_{n-1}^* - U_{n-1} \right|\!\right|\!\right|^2$.
- **Time error indicator:**
$$\mathcal{E}_\tau^2(n) = 2\tau_n \left|\!\left|\!\left| U_{n-1}^* - U_n \right|\!\right|\!\right|^2. \tag{4.1}$$
- **Spatial error indicator:** We consider, for each $\beta \in \mathcal{H}_n$,
$$\mathcal{E}^2_{\mathcal{H}_n}(\beta) := \tau_n C_U a_\beta h_\beta^2 \int_{\operatorname{supp}\beta} |f - \frac{1}{\tau_n}(U_n - U_{n-1}^*) + \operatorname{div}(\mathcal{A}\nabla U_n) - cU_n|^2 \beta,$$
where $U_n \in \mathbb{V}_n$ is the solution of the discrete elliptic problem
$$\langle \frac{1}{\tau_n} U_n, V\rangle_\Omega + B[U_n, V] = \langle \frac{1}{\tau_n} U_{n-1}^* + f_n, V\rangle_\Omega, \quad \forall\, V \in \mathbb{V}_n.$$
If $u_n \in H_0^1(\Omega)$ is the weak solution to the elliptic equation
$$-\operatorname{div}(\mathcal{A}\nabla u_n) + \left(c + \frac{1}{\tau_n}\right) u_n = f + \frac{1}{\tau_n} U_{n-1}^* \quad \text{in } \Omega, \qquad u_n = 0 \quad \text{on } \partial\Omega, \tag{4.2}$$
then $\{\mathcal{E}_{\mathcal{H}_n}(\beta)\}_{\beta\in\mathcal{H}_n}$ are the local error estimators from Buffa and Garau (2018) corresponding to this elliptic problem and $\tau_n |\!|\!| u_n - U_n |\!|\!| \le \left(\sum_{\beta\in\mathcal{H}_n} \mathcal{E}^2_{\mathcal{H}_n}(\beta)\right)^{\frac{1}{2}} =: \mathcal{E}_{\mathcal{H}}(n)$.
- **Interpolation error indicator:** $\mathcal{E}_{\mathcal{I}}^2(n) = \|U_{n-1} - U_{n-1}^*\|^2_{H^{-1}(\Omega)}$.
- **Consistency error indicator:** $\mathcal{E}_f^2(n) = \int_{I_n} \|f - f_n\|^2_{L^2(\Omega)}\, dt$.

The total error is bounded by the above defined error indicators, as stated in the following theorem, whose proof follows the same lines in (Gaspoz et al., 2018, Proposition 3.4).

Theorem 4.1. *Let u be the weak solution to problem (1.1) and let $\mathcal{U}$ be the discrete solution defined by (3.2). Then,*

$$\|u - \mathcal{U}\|^2_{\mathbb{W}(0,T)} \le \mathcal{E}_0^2 + \sum_{n=1}^{N} \mathcal{E}_\tau^2(n) + \mathcal{E}_c^2(n) + \mathcal{E}^2_{\mathcal{H}}(n) + \mathcal{E}^2_{\mathcal{I}}(n) + \mathcal{E}_f^2(n). \tag{4.3}$$

5 CONTROLLING THE CONSISTENCY ERROR INDICATOR

The following result is a consequence of (Gaspoz et al., 2018, Lemma 4.4) and allows us to control the consistency error indicator.

Theorem 5.1. *Given* $f \in L^2(0,T;L^2(\Omega))$ *and* $\mathrm{TOL}_f > 0$, *let* $0 = s_0 < s_1 < \cdots < s_M = T$ *be a partition of* $[0,T]$ *such that*

$$\sum_{m=1}^{M} \int_{s_{m-1}}^{s_m} \|f - f_{[s_{m-1},s_m)}\|^2 dt \leq \frac{\mathrm{TOL}_f^2}{2}, \qquad \textit{with} \quad f_{[s_{m-1},s_m)} := \fint_{[s_{m-1},s_m)} f(t)\,dt. \tag{5.1}$$

Let $\mathrm{tol}_f^2 := \frac{\mathrm{TOL}_f^2}{2(M-1)}$. *If* $0 = t_0 < t_1 < \cdots < t_N = T$ *is any partition of* $[0,T]$ *that satisfies*

$$\int_{t_{n-1}}^{t_n} \|f - f_{[t_{n-1},t_n)}\|^2 dt \leq \mathrm{tol}_f^2, \qquad n = 1,2,\ldots,N, \tag{5.2}$$

then,

$$\sum_{n=1}^{N} \int_{t_{n-1}}^{t_n} \|f - f_{[t_{n-1},t_n)}\|^2 dt \leq \mathrm{TOL}_f^2\,. \tag{5.3}$$

Remark 1. Given $\mathrm{TOL}_f > 0$, it is easy to build a partition $0 = s_0 < s_1 < \cdots < s_M = T$ satisfiying (5.1). Using a *greedy* algorithm we even obtain a quasi-optimal partition; see Algorithm 1. This algorithm entails a substantial improvement over the **TOLFIND** algorithm presented in Gaspoz et al. (2018), which is very expensive from the computational viewpoint.

Algorithm 1 compute_local_tolerance

Input: f, T, TOL_f
$e^2 = \int_0^T \|f - f_{[0,T]}\|^2_{L^2(\Omega)}$
Partition $= \{0,T\}$ % ($s_0 = 0$, $s_1 = T$)
$M = 1$; % Number of sub-intervals
while $e^2 > \frac{\mathrm{TOL}_f^2}{2}$ **do**
  $i = \arg\max_{1\leq j\leq M} \int_{s_{j-1}}^{s_j} \|f - f_{[s_{j-1},s_j]}\|^2_{L_2(\Omega)}$
  Partition $\leftarrow$ Partition $\cup \left\{\frac{s_{i-1}+s_i}{2}\right\}$ % Insert $\frac{s_{i-1}+s_i}{2}$ as a partition point.
  $M \leftarrow M + 1$;
  $e^2 = \sum_{j=1}^{M} \int_{s_{j-1}}^{s_j} \|f - f_{[s_{j-1},s_j]}\|^2_{L_2(\Omega)}$
end while
$\mathrm{tol}_f = \sqrt{\frac{\mathrm{TOL}_f^2}{2\max(1,M-1)}}$;
end
Output: tol_f

Remark 2. Given $f \in L^2(0,T;L^2(\Omega))$ and tol_f, there is a lower bound on τ in order to fulfill (5.2). In fact, if $0 = t_0 < t_1 < \cdots < t_N = T$ is a partition of $[0,T]$ satisfying $\int_{t_{n-1}}^{t_n} \|f - f_{[t_{n-1},t_n)}\|^2 dt \leq \mathrm{tol}_f^2/2$, $n = 1,2,\ldots,N$, then for any interval $I \subset [0,T]$ with $|I| \leq \tau_* := \min_{n=1,\ldots,N} t_n - t_{n-1}$ we have $\int_I \|f - f_I\|^2\,dt \leq \mathrm{tol}_f^2$.

6 CONTROLLING THE TIME ERROR INDICATOR

The next result follows the same lines as in Corollary 3.4 from Kreuzer et al. (2012).

Theorem 6.1. *Let $N \in \mathbb{N}$ and $\{t_n\}_{n=0}^N$ be arbitrary time instances. Let $\tau_n := t_n - t_{n-1}$ be the time step sizes and $U_n \in \mathbb{V}_n$ be the discrete solutions of (3.1), with $U_{n-1}^* \in \mathbb{V}_n$ satisfying*

$$\left|\left|\left| U_{n-1}^* \right|\right|\right|^2 - \left|\left|\left| U_{n-1} \right|\right|\right|^2 \leq \tau_{n-1}, \qquad n = 2, \ldots, N. \tag{6.1}$$

Then,

$$\sum_{n=1}^{N} \left|\left|\left| U_n - U_{n-1}^* \right|\right|\right|^2 \leq \|f\|^2_{\Omega\times(0,t_N)} + \left|\left|\left| U_0 \right|\right|\right|^2 + T. \tag{6.2}$$

We have also the following auxiliary result, whose proof follows as in (Kreuzer et al., 2012, Proposition 3.3).

Lemma 6.2. *Let $N \in \mathbb{N} \cup \{\infty\}$ and $0 = t_0 < t_1 < \cdots < t_N \leq T$ be arbitrary time instances. Let $\tau_n := t_n - t_{n-1}$ be the time step sizes and $U_n \in \mathbb{V}_n$ be the discrete solution of (3.1), with $U_{n-1}^* \in \mathbb{V}_n$, for $n = 1, 2, \ldots, N$. Then, for $m = 1, \ldots, N$, there holds*

$$\sum_{n=1}^{m} \frac{1}{\tau_n} \|U_n - U_{n-1}^*\|^2 + \left|\left|\left| U_n - U_{n-1}^* \right|\right|\right|^2 + \left|\left|\left| U_n \right|\right|\right|^2 - \left|\left|\left| U_{n-1}^* \right|\right|\right|^2 \leq \|f\|^2_{\Omega\times(0,t_m)}.$$

7 ADAPTIVE ALGORITHM

We now present the main adaptive algorithm, which constructs a sequence of time instants $0 = t_0 < t_1 < \cdots < t_N = T$ and discrete approximations U_n, so that the right-hand side of (4.3) is bounded by the desired tolerance.

The main algorithm is **ASTIGM** (Algorithm 2), and consists of the following steps.

- First, the tolerance TOL is split into three parts TOL_0, TOL_f and TOL_Q to account for the different sources of error. TOL_0 will bound the approximation of the initial data, TOL_f will be used as an input fo the routine **compute_local_tolerance** to set a local tolerance for controlling the consistency error indicator. TOL_Q will be an upper bound for the errors due to time and space discretization, and properly scaled will be the input of **space_and_time_adaptation** (Algorithm 3).

- Given $\mathrm{TOL}_f > 0$ we first compute $\mathrm{tol}_f > 0$ using the routine **compute_local_tolerance** as explained in Section 5, such that $\mathcal{E}_f^2(n) \leq \mathrm{tol}_f^2$, $n = 1, 2, \ldots, N \implies \sum_{n=1}^N \mathcal{E}_f^2(n) \leq \mathrm{TOL}_f^2$.

- We next call the module **consistency** which just sets τ_1 as an upper bound for the first timestep so that $\mathcal{E}_f(1) = \left(\int_{t_0}^{t_0+\tau_1} \|f - f_1\|^2_{L^2(\Omega)}\, dt \right)^{\frac{1}{2}} \leq \mathrm{tol}_f$ holds.

- The initialization step ends with a call to **adapt_initial_mesh**, which adaptively refines the mesh $\mathcal{Q}_{\text{init}}$ to get $\mathcal{Q}_0 = \mathcal{Q}_0^*$ and $U_0 = U_0^* \in \operatorname{span} \mathcal{H}_0$, where $\mathcal{H}_0 = \mathcal{H}_0^*$ is the hierarchical basis corresponding to $\mathcal{Q}_0$, such that

$$\|u_0 - U_0\| \leq \mathrm{TOL}_0\,. \tag{7.1}$$

- Next, we repeat the following steps.

– Given a mesh $\mathcal{Q}^*_{n-1}$, a hierarchical basis $\mathcal{H}^*_{n-1}$, and the corresponding $U^*_{n-1} \in \operatorname{span} \mathcal{H}^*_{n-1}$ at time t_{n-1}, and an initial guess τ_n satisfying

$$\mathcal{E}_f(n) = \Big(\int_{t_{n-1}}^{t_{n-1}+\tau_n} \|f - f_n\|^2_{L^2(\Omega)}\, dt \Big)^{\frac{1}{2}} \leq \mathrm{tol}_f, \tag{7.2}$$

we determine adaptively a time step τ_n and a mesh $\mathcal{Q}_n$ associated to $t_n := t_{n-1} + \tau_n$. This is done inside the module **space_and_time_adaptation**, detailed in Algorithm 3 below. It reduces the time step τ_n and refines the mesh $\mathcal{Q}^*_{n-1}$ (if necessary) giving rise to the mesh $\mathcal{Q}_n$ in order to guarantee that $\mathcal{E}^2_\tau(n) + \mathcal{E}^2_{\mathcal{H}}(n)$ is small enough. More specifically, we start with the initial guess τ_n as large as possible such that (7.2) holds, and in this module we will eventually reduce τ_n to decrease the other error indicators; we notice that $\mathcal{E}_f(n)$ will not increase as τ_n is reduced, so that (7.2) will continue to hold. Also, we start with a candidate mesh $\mathcal{Q}_n = \mathcal{Q}^*_{n-1}$ obtained from a coarsening of $\mathcal{Q}_{n-1}$, and in this module we will update $\mathcal{Q}_n$ only by refinement.

– We next call **consistency** to compute the *largest* time step τ_{n+1} such that (7.2) holds for $n+1$.

– Finally, in the module **coarsen** we de-refine the mesh $\mathcal{Q}_n$ and obtain a coarser mesh $\mathcal{Q}^*_n$ and an approximation U^*_n such that

$$\mathcal{E}^2_{\mathcal{I}}(n+1) + \mathcal{E}^2_c(n+1) \leq \mathcal{E}^2_\tau(n) + \mathcal{E}^2_f(n) + \tau_n \,\mathrm{tol} \quad \text{and} \quad |||U^*_n|||^2 - |||U_n|||^2 \leq \tau_n. \tag{7.3}$$

Thus, no extra refinement will be needed to control $\mathcal{E}^2_{\mathcal{I}}(n+1)$ and $\mathcal{E}^2_c(n+1)$ after reducing τ_{n+1} or refining the space, and the estimate (6.2) holds; **coarsen** can now fix the initial term U^*_n of the n-th step without the need to modify it later, allowing us to discard $\mathcal{Q}_n$ from memory.

Algorithm 2 ASTIGM: Adaptive space-time isogeometric method

Input: $\mathcal{Q}_{\text{init}}$, $\mathrm{TOL} > 0$
$t_0 = 0$
$n = 0$
Split TOL such that $\mathrm{TOL}^2 = \mathrm{TOL}_0^2 + 3\,\mathrm{TOL}_f^2 + \mathrm{TOL}_{\mathcal{Q}}^2$.
$\mathrm{tol}_f =$ **compute_local_tolerance** (f, T, TOL_f)
$\tau_1 =$ **consistency** $(f, t_0, T, \mathrm{tol}_f)$
$[U^*_0, \mathcal{Q}^*_0] = [U_0, \mathcal{Q}_0] =$ **adapt_initial_mesh** $(u_0, \mathcal{Q}_{\text{init}}, \mathrm{TOL}_0)$
while $t_n < T$ **do**
    $n \leftarrow n+1$
    $[U_n, \tau_n, f_n, \mathcal{Q}_n] =$ **space_and_time_adaptation** $(U^*_{n-1}, f, t_{n-1}, \tau_n, \mathcal{Q}^*_{n-1}, \mathrm{TOL}^2_{\mathcal{Q}}/C_T)$
    $t_n = t_{n-1} + \tau_n$
    $\tau_{n+1} = \min\{\tau_n, T - t_n\}$
    $\tau_{n+1} =$ **consistency** $(f, t_n, \tau_{n+1}, \mathrm{tol}_f)$
    $[\mathcal{Q}^*_n, U^*_n] =$ **coarsen** $(U_n, \mathcal{Q}_n, \tau_n)$
end while
end

Algorithm 3 space_and_time_adaptation: Adapt the time step τ_n and refine the mesh $\mathcal{Q}_n$ in order to guarantee that $\mathcal{E}_\tau^2(n) + \mathcal{E}_{\mathcal{H}}^2(n)$ are small enough

Input: $V_{n-1}, f, t_{n-1}, \tau_n, \mathcal{Q}_n, \mathrm{tol}_{\mathcal{Q}}$, fixed parameter $\kappa \in (0,1)$
1: Compute $\mathcal{E}_f^2(n)$
2: **while** 1 **do**
3: $I_n = [t_{n-1}, t_{n-1} + \tau_n]$
4: $U_n =$ **solve** $(V_{n-1}, f_n, \tau_n, \mathcal{Q}_n)$ % see (3.1)
5: Compute $\mathcal{E}_{\mathcal{H}}^2(n), \mathcal{E}_\tau^2(n)$
6: **if** $\mathcal{E}_\tau^2(n) > \mathrm{tol}_{\mathcal{Q}}^2$ **then**
7: $\tau_n = \kappa\tau_n$ % reduce the time step τ_n
8: Compute $\mathcal{E}_f^2(n)$
9: **else if** $\mathcal{E}_{\mathcal{H}}^2(n) > \mathcal{E}_\tau^2(n) + \mathcal{E}_f^2(n) + \tau_n \mathrm{tol}_{\mathcal{Q}}$ **then**
10: $\mathcal{Q}_n =$ **mark_and_refine** $(\{\mathcal{E}_{\mathcal{H}_n}(\beta)\}_{\beta\in\mathcal{H}_n}, \mathcal{Q}_n)$
11: **else**
12: **break**
13: **end if**
14: **end while**
Output: $U_n, \tau_n, f_n, \mathcal{Q}_n$

8 CONVERGENCE ANALYSIS FOR ASTIGM

Proposition 8.1 (Termination of ASTIGM)**.** *The adaptive algorithm ASTIGM terminates in finite time and produces a finite number of time instances* $0 = t_0 < t_1 < t_2 < \cdots < t_N = T$*, meshes* $\mathcal{Q}_n$ *and approximations* $U_n \in \operatorname{span}\mathcal{H}_n$ *such that*

$$\begin{cases} \mathcal{E}_0 \le \mathrm{TOL}_0, \qquad \displaystyle\sum_{n=1}^{N} \mathcal{E}_f^2(n) \le \mathrm{TOL}_f^2, \\ \mathcal{E}_\tau^2(n) \le \mathrm{tol}_{\mathcal{Q}}^2, \quad \mathcal{E}_{\mathcal{H}}^2(n) \le \mathcal{E}_\tau^2(n) + \mathcal{E}_f^2(n) + \tau_n \mathrm{tol}_{\mathcal{Q}}, \qquad n = 1, 2, \ldots, N, \\ \mathcal{E}_c^2(n+1) + \mathcal{E}_{\mathcal{I}}^2(n+1) \le \mathcal{E}_\tau^2(n) + \mathcal{E}_f^2(n) + \tau_n \mathrm{tol}_{\mathcal{Q}}, \quad n = 1, \ldots, N-1. \end{cases}$$

where $\mathrm{tol}_{\mathcal{Q}} = \frac{\mathrm{TOL}_{\mathcal{Q}}^2}{C_T}$ *and* $C_T = \left[9\sqrt{T}\left(\|f\|_{L^2(\Omega\times(0,T))}^2 + |||U_0|||^2 + T\right)^{\frac{1}{2}} + 2T\right]$ *(see Theorem 8.2).*

Proof. The call to **compute_local_tolerance** guarantees that tol_f satisfies Theorem 5.1. Afterwards, **ASTIGM** calls the module **consistency** which selects $\tau_1 > \tau_*$ such that (7.2) is satisfied. The call to **adapt_initial_mesh** guarantees that the initial error satisfies $\mathcal{E}_0 \le \mathrm{TOL}_0$.

The **while** loop inside **ASTIGM** calls first the module **space_and_time_adaptation** which starts with $\mathcal{Q}_n = \mathcal{Q}_{n-1}^*$ and τ_n as the output of the last call to *consistency*, and entails another **while** loop (Algorithm 3). Each iteration of this inner loop consists of two steps. First, a discrete solution U_n to (3.1) is computed on the current mesh $\mathcal{Q}_n$ with the current time-step size τ_n. Next, either the time step-size is reduced (if $\mathcal{E}_\tau(n) > \mathrm{tol}_{\mathcal{Q}}$) or the actual grid is refined (if $\mathcal{E}_\tau(n) \le \mathrm{tol}_{\mathcal{Q}}$ and $\mathcal{E}_{\mathcal{H}}^2(n) > \mathcal{E}_\tau^2(n) + \mathcal{E}_f^2(n) + \tau_n \mathrm{tol}_{\mathcal{Q}}$). This is the only step of the algorithm where τ_n could be reduced below τ_*. But notice that τ_n is only reduced if $\mathcal{E}_\tau(n) > \mathrm{tol}_{\mathcal{Q}}$, i.e., if

$$\frac{1}{\tau_n} < \frac{1}{\tau_n}\frac{\mathcal{E}_\tau^2(n)}{\mathrm{tol}_{\mathcal{Q}}^2} = \frac{2\tau_n |||U_{n-1}^* - U_n|||^2}{\tau_n \mathrm{tol}_{\mathcal{Q}}^2} \le \frac{2}{\mathrm{tol}_{\mathcal{Q}}^2}\left(\|f\|_{L^2(\Omega\times(0,T))}^2 + \|\nabla U_0\|^2 + T\right)$$

due to Theorem 6.1. This implies that always $\tau_n \ge \frac{\kappa}{2}\frac{\mathrm{tol}_{\mathcal{Q}}^2}{\|f\|_{L^2(\Omega\times(0,T))}^2 + \|\nabla U_0\|^2 + T}$, and also, that line 7 of **space_and_time_adaptation** is executed finitely many times. Due to the fact that the

adaptive algorithm for elliptic problems **mark_and_refine** converges into tolerance in finite steps, also line 10 is executed a finite number of times, whence the **while** loop ends in finite time.

When **space_and_time_adaptation** ends, **ASTIGM** calls the module **consistency** which selects a timestep τ_n such that (7.2) is satisfied, but according to Remark 2, either $\tau_n > \tau_*$ or $t_n = T$. This sets the maximum timestep for this n and thanks to the choice of tol_f, the overall consistency error will be bounded by TOL_f. Finally, the module **coarsen** leads to a mesh $\mathcal{Q}_n^*$ with an associated hierarchical basis $\mathcal{H}_n^*$ such that $\operatorname{span}\mathcal{H}_n^* \subset \operatorname{span}\mathcal{H}_{n-1}$ and (7.3) is satisfied.

Since every **space_and_time_adaptation** ends in finite steps and $\tau_n > \tau_*$, the final time is reached. The estimates follow from the fact that the **break** statement is executed in both algorithms, whence $\mathcal{E}_\tau(n) \leq \mathrm{tol}_\mathcal{Q}$, $\mathcal{E}_\mathcal{H}^2(n) \leq \mathcal{E}_\tau^2(n) + \mathcal{E}_f^2(n) + \tau_n\,\mathrm{tol}_\mathcal{Q}$ and (7.3) holds. □

Theorem 8.2 (Convergence into tolerance)**.** *The algorithm ASTIGM computes a suitable partition* $0 = t_0 < t_1 < t_2 < \cdots < t_N = T$ *and for each* $n = 1, 2, \ldots, N$*, the discrete value* $U_n \in \operatorname{span}\mathcal{H}_n$*, where* $\mathcal{H}_n$ *is the hierarchical basis associated to a hierarchical mesh* $\mathcal{Q}_n$ *such that*

$$\|u - \mathcal{U}\|_{\mathbb{W}(0,T)} \leq \mathrm{TOL},$$

where $\mathcal{U} \in \mathbb{W}(0,T)$ *is the discrete approximation of* u *obtained from* $\{U_n\}_{n=0}^N$ *through* (3.2)*.*

Proof. From Theorem 4.1 we only need to bound the term $\mathbf{E} := \sum_{n=1}^N \Big[\mathcal{E}_\tau^2(n) + \mathcal{E}_c^2(n) + \mathcal{E}_\mathcal{H}^2(n) + \mathcal{E}_\mathcal{I}^2(n) + \mathcal{E}_f^2(n)\Big]$, which, due to Proposition 8.1 satisfies

$$\mathbf{E} \leq \sum_{n=1}^N \Big[3\mathcal{E}_\tau^2(n) + 3\mathcal{E}_f^2(n) + 2\tau_n\,\mathrm{tol}_\mathcal{Q}\Big] \leq 3\sum_{n=1}^N \mathcal{E}_\tau^2(n) + 3\,\mathrm{TOL}_f^2 + 2T\,\mathrm{tol}_\mathcal{Q}\,.$$

Using (4.1), (6.2) and Proposition 8.1 we get, for $\delta = \left(\frac{T}{\|f\|^2_{L^2(\Omega\times(0,T))} + |||U_0|||^2 + T}\right)^{\frac{1}{2}} \frac{\mathrm{tol}_\mathcal{Q}}{2}$,

$$\begin{aligned}\sum_{n=1}^N \mathcal{E}_\tau^2(n) &= \sum_{\tau_n > \delta} \mathcal{E}_\tau^2(n) + \sum_{\tau_n \leq \delta} \mathcal{E}_\tau^2(n) \leq \frac{T}{\delta}\,\mathrm{tol}_\mathcal{Q}^2 + 2\delta \sum_{n=1}^N \big|\!\big|\!\big| U_n - U_{n-1}^* \big|\!\big|\!\big|^2 \\ &\leq \frac{T}{\delta}\,\mathrm{tol}_\mathcal{Q}^2 + 2\delta\left(\|f\|^2_{L^2(\Omega\times(0,T))} + |||U_0|||^2 + T\right) \\ &\leq 3\sqrt{T}\left(\|f\|^2_{L^2(\Omega\times(0,T))} + |||U_0|||^2 + T\right)^{\frac{1}{2}} \mathrm{tol}_\mathcal{Q}\,.\end{aligned}$$

Finally, $\mathbf{E} \leq \underbrace{\left[9\sqrt{T}\left(\|f\|^2_{L^2(\Omega\times(0,T))} + |||U_0|||^2 + T\right)^{\frac{1}{2}} + 2T\right]}_{=C_T} \mathrm{tol}_\mathcal{Q} + 3\,\mathrm{TOL}_f^2 = \mathrm{TOL}_\mathcal{Q}^2 + 3\,\mathrm{TOL}_f^2$, which proves the assertion. □

9 NUMERICAL TESTS

We present two numerical tests to assess the efficiency of the method. In both cases, and for simplicity, in problem (1.1) we set $c = 0$ and $\mathcal{A} = \mathbb{I}$ is the identity matrix, the spatial domain is $\Omega = (-1,1)^2$, and the final time is set to $T = 1$.

For the discretization, we use biquadratic hierarchical B-splines with C^1 continuity, which allows to neglect the jump terms across elements in the spatial estimators. We use the spatial

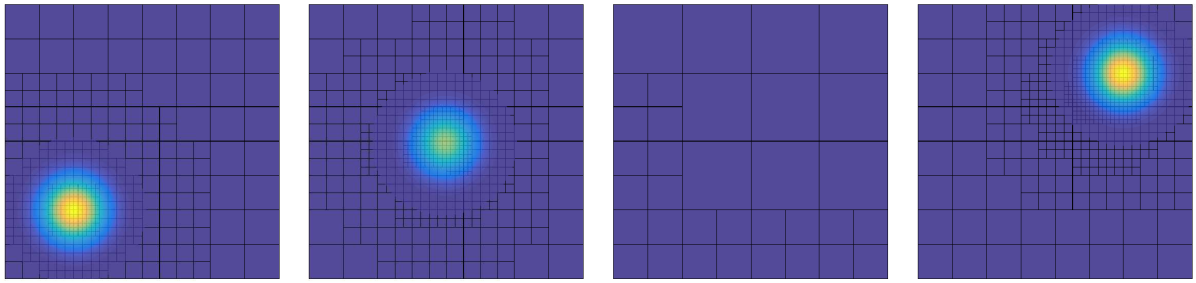

Figure 1: Meshes and approximated solution at times $t \approx 3 \cdot 10^{-4}$, $t \approx 0.49$, $t \approx 0.5$, $t = 1$. The finest level of the hierarchical mesh at each step is, respectively, 6, 6, 3 and 6, and the number of elements is 427, 553, 34 and 673.

a posteriori error estimator introduced in Buffa and Garau (2018) for hierarchical B-splines, and for spatial refinement we use the maximum strategy, with parameter equal to 0.5 for refinement. For coarsening, the first coarsening step is done using a minimum strategy based on the spatial estimator, with a parameter equal to 0.75, and refinements of this coarsened mesh are obtained based on the coarsening estimator. The method is implemented in the Matlab code GeoPDEs, see Vázquez (2016), using the same algorithms and data structures detailed in Garau and Vázquez (2018) for refinement. For coarsening, from the set of marked functions we mark active elements such that all the functions of its level have been marked, and then de-refine an element if all its children are marked. This guarantees that non-marked functions will remain active, see also Carraturo et al. (2019). During coarsening, the approximation U^*_{n-1} is computed as the L^2 projection of U_{n-1} into the coarsened mesh, and the estimator $\mathcal{E}_{\mathcal{I}}$ is replaced by the term $\|U_{n-1} - U^*_{n-1}\|_{L^2(\Omega)}$.

Example 1: moving peak. As a first numerical test we use the same example presented in Chen and Feng (2004), see also Kreuzer et al. (2012). The right-hand side f, the boundary condition and the initial data u_0 are chosen such that the exact solution of the continuous problem is given by

$$u(x,t) = \alpha(t) e^{-\beta[(x_1 - t + 0.5)^2 + (x_2 - t + 0.5)^2]}, \text{ with } \alpha(t) = (1 - e^{-\gamma(t-0.5)^2}),$$

with the constants $\beta = 25$ and $\gamma = 10^4$. The solution consists of a peak that moves at constant speed along the diagonal of the square domain Ω, with a rapid exponential drop before time $t = 0.5$. At that time the solution flattens to a constant zero value, and then it experiences a rapid exponential recovery.

We choose the parameters $\mathrm{TOL}_0^2 = 10^{-6}$ and $\mathrm{TOL}_f^2 = 10^{-3}$, and $\mathrm{TOL}_{\mathcal{Q}}$ is chosen such that $\mathrm{tol}_{\mathcal{Q}}^2 = 10^{-3}$. In Figure 1 we present several meshes and the corresponding solutions at different time steps, which show how the mesh adequately follows the moving peak, applying coarsening after the peak has passed by, and also when the solution is flattened to zero.

In Figure 2(a) we plot the number of degrees of freedom and the time step sizes. We observe that both quantities remain almost constant during the simulation, except around $t = 0.5$ where the mesh is coarsened and the time step needs to be refined. Moreover, we show in Figure 2(b) the value of the time, space and consistency error indicators, along with the total one.

Example 2: rough initial data. The second example is taken from Kreuzer et al. (2012), and considers a problem with homogeneous boundary conditions and rough initial data. We use a

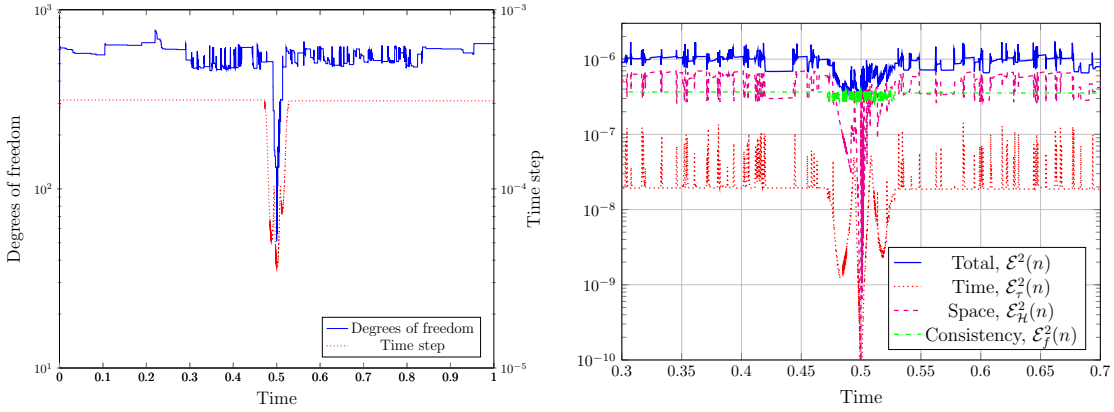

(a) Time step and degrees of freedom.

(b) Estimators.

Figure 2: Results of the example of the moving peak.

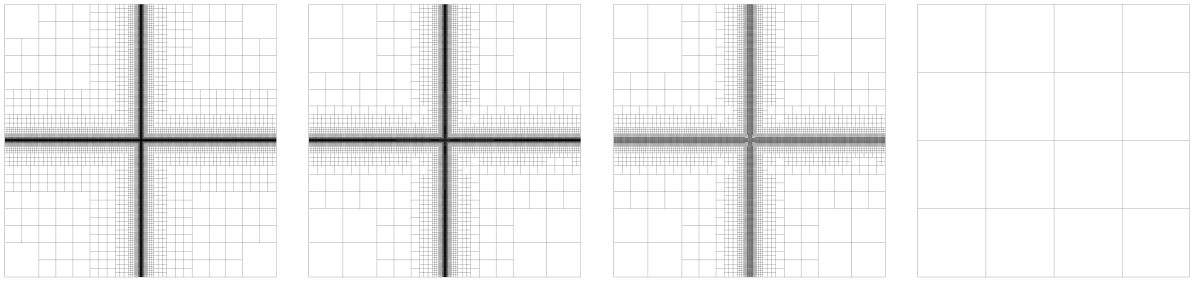

Figure 3: Meshes at times $t \approx 2 \cdot 10^{-7}$, $t \approx 10^{-4}$, $t \approx 10^{-3}$, $t = 1$. The finest level of the hierarchical mesh at each step is, respectively, 11, 11, 9 and 2, and the number of elements is 60412, 52954, 17299 and 16.

vanishing load function $f \equiv 0$ and as initial data a function with checkerboard pattern in Ω, and which is given by the values $u_0 \equiv 1$ in $\Omega_1 = (-1, 0) \times (0, 1) \cup (0, 1) \times (-1, 0)$, and $u_0 \equiv 0$ in $\Omega \setminus \Omega_1$. During time evolution, the jumps of the initial data are smoothed out, and the solution tends to a constant steady state, which however is still not reached at time $T = 1$.

As in Kreuzer et al. (2012) we choose $\mathrm{TOL}_0^2 = 10^{-3}$ in (7.1), and $\mathrm{TOL}_f^2 = 10^{-3}$, although this is not relevant because $f = 0$. The other tolerance is chosen such that $\mathrm{tol}_{\mathcal{Q}}^2 = 8 \cdot 10^{-3}$. In Figure 3 we depict four meshes at different time steps, which show how the mesh is initially refined at the discontinuity regions, and then it tends to be coarsened until it becomes uniform. In Figure 4(a) we plot the number of degrees of freedom and the time step, which confirms that both the mesh and the time step sizes are coarsened during the simulation. Finally, we plot in Figure 4(b) the evolution of the total error indicator, along with the time and spatial error indicators. As can be seen, the time error indicator is the one who contributes the most to the total error indicator. There are however some steps, corresponding to peaks in the total error, in which the coarsening and interpolation error indicators (not shown) give a more important contribution.

ACKNOWLEDGEMENTS

The work of E.M.G. and P.M. was partially supported by Agencia Nacional de Promoción Científica y Tecnológica, through grants PICT-2014-2522, PICT-2016-1983, by CONICET through PIP 2015 11220150100661, and by Universidad Nacional del Litoral through CAI+D

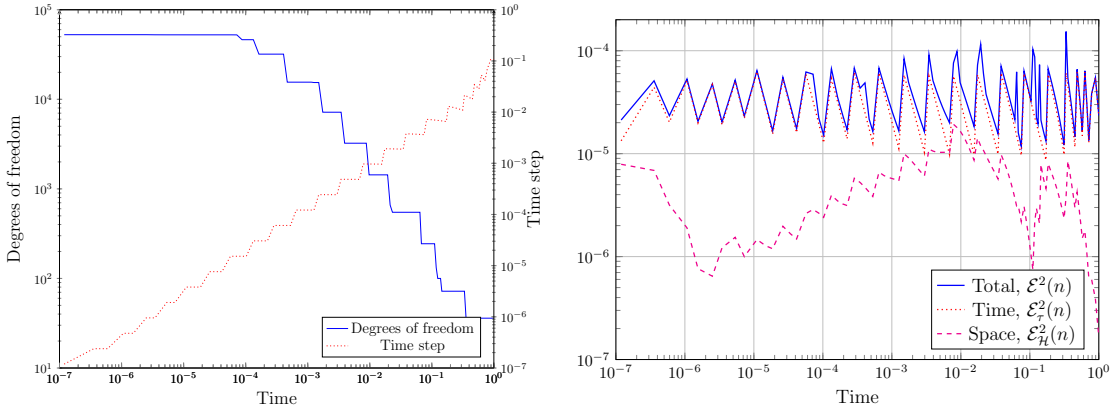

(a) Time step and degrees of freedom. (b) Estimators.

Figure 4: Results of the example with rough initial data.

2016-50420150100022LI.

The work of F.D.G. was partially supported by the DFG project 814/7-1.

The work of R.V. was partially supported by the ERC AdG project CHANGE n. 694515.

REFERENCES

Buffa A. and Garau E.M. A posteriori error estimators for hierarchical B-spline discretizations. *Math. Models Methods Appl. Sci.*, 28(8):1453–1480, 2018. ISSN 0218-2025. doi:10.1142/S0218202518500392.

Carraturo M., Giannelli C., Reali A., and Vázquez R. Suitably graded THB-spline refinement and coarsening: towards an adaptive isogeometric analysis of additive manufacturing processes. *Comput. Methods Appl. Mech. Engrg.*, 348:660–679, 2019. ISSN 0045-7825. doi:10.1016/j.cma.2019.01.044.

Chen Z. and Feng J. An adaptive finite element algorithm with reliable and efficient error control for linear parabolic problems. *Math. Comp.*, 73(247):1167–1193, 2004. ISSN 0025-5718. doi:10.1090/S0025-5718-04-01634-5.

Garau E.M. and Vázquez R. Algorithms for the implementation of adaptive isogeometric methods using hierarchical B-splines. *Appl. Numer. Math.*, 123:58–87, 2018. ISSN 0168-9274. doi:10.1016/j.apnum.2017.08.006.

Gaspoz F.D., Kreuzer C., Siebert K.G., and Ziegler D.A. A convergent time–space adaptive dG(s) finite element method for parabolic problems motivated by equal error distribution. *IMA J. Numer. Anal.*, 39(2):650–686, 2018. doi:https://doi.org/10.1093/imanum/dry005.

Kreuzer C., Möller C.A., Schmidt A., and Siebert K.G. Design and convergence analysis for an adaptive discretization of the heat equation. *IMA J. Numer. Anal.*, 32(4):1375–1403, 2012. ISSN 0272-4979. doi:10.1093/imanum/drr026.

Vázquez R. A new design for the implementation of isogeometric analysis in Octave and Matlab: GeoPDEs 3.0. *Comput. Math. Appl.*, 72(3):523–554, 2016. ISSN 0898-1221. doi:10.1016/j.camwa.2016.05.010.